Upper Ocean Heat Budget During the Hawaii-to-Tahiti Shuttle Experiment

JAMES W. STEVENSON AND PEARN P. NIILER[1]

Joint Institute for Marine and Atmospheric Research, University of Hawaii, Honolulu, HI 96822

(Manuscript received 20 December 1982, in final form 22 April 1983)

ABSTRACT

Heat flux, CTD and current profile data from the Hawaii-to-Tahiti Shuttle Experiment are used to study the upper ocean heat budget in order to better understand the seasonal evolution of sea surface temperature (SST) in the central tropical Pacific Ocean between February 1979 and June 1980. The surface heat flux is estimated using bulk formulas and the standard meteorological data taken aboard ship. Upper ocean heat storage is computed from CTD data in such a way (using temperature vertically averaged between the sea surface and fixed isotherm depths) as to filter internal waves. It is found that the surface heat flux plays a large role in the seasonal evolution of SST. A time–latitude correlation coefficient of 0.70 is found between the surface heat flux and heat storage. The seasonal evolution of the vertically averaged temperature whose time rate of change determines storage is very closely correlated with the seasonal evolution of SST.

At 155°W, there is no evidence for a relation between changes of main thermocline depths and changes in SST. Also, we see no feedback from the ocean to the atmosphere through SST governed heat flux. Horizontal heat advection is estimated from Firing *et al.* profiling current meter data. The advection of cold water from the east is important in the 15-cruise (16-month) mean but the data are too noisy to estimate the seasonal evolution of heat advection.

1. Introduction

Gaining an understanding of the processes which cause the low-frequency variation of the tropical Pacific Ocean sea surface temperature (SST) is a useful contribution to an understanding of global climate. A number of researchers have found evidence that anomalies of SST in the tropical Pacific Ocean appear to be related to several aspects of global climate. Newell *et al.* (1978) found a relationship between the time-varying coefficient of the first mode nonseasonal empirical orthogonal function for Pacific Ocean SST and atmospheric CO_2 changes at the South Pole. Several researchers have statistically related anomalies of SST in the central and eastern tropical Pacific Ocean to North American winter climate. Horel and Wallace (1981) found a contemporaneous correlation between wintertime SST anomalies in the central tropical Pacific and the wintertime 700 mb height field over North America. Barnett (1981) found that SST anomalies in the eastern tropical Pacific could be used to improve predictability of wintertime air temperatures over the southeastern, western and northern United States and southern Canada. There have also been model studies (e.g., Webster, 1981; Hoskins and Karoly, 1981) which show that SST or heat flux anomalies in the tropics force long-wavelength atmospheric Rossby waves that propagate poleward and eastward. The important unanswered question is whether the ocean acts to store heat passively as it appears to be in the northeastern Pacific (Davis, 1976, 1978) or whether its internal dynamical processes determine the release of heat and moisture back to the atmosphere through changes of SST.

There are many processes that determine SST variations in the tropics. Perhaps the most obvious process is the surface heat flux: the incoming shortwave solar radiation less the sum of the outgoing longwave radiation latent heat flux and sensible heat flux. McPhaden (1982) found that in a two-year record local storage of the surface heat flux accounted for 80% of the variance of SST in the central Indian Ocean (00°41′S, 73°10′E). A second process which affects SST is a combination of vertical advection and vertical mixing. The SST decreases when cool water is upwelled and mixed with the water near the sea surface. Wyrtki (1981) discusses the role of upwelling in maintaining the long-term mean tongue of cool water along the equator in the eastern Pacific Ocean. Niiler and Stevenson (1982) show that on the long-term mean, vertical diffusion is important in the upper ocean heat budget in the tropical Atlantic and Pacific Oceans. The vertical motions in the upper ocean associated with equatorially trapped waves can potentially affect SST as well. A number of equatorial modelers have assumed a relationship between isotherm or layer depths in their models and SST and in this way, adiabatic motions of the main thermocline are thought to affect the sea surface temperature

[1] Present affiliation: Scripps Institution of Oceanography, A-030, La Jolla, CA 92093.

(e.g., Busalacchi and O'Brien, 1981). Horizontal advection is a third process which can affect SST. Wyrtki (1981) discusses the role of horizontal advection by the South Equatorial Current in maintaining the cool tongue in the tropical Pacific. The role of horizontal heat advection in warming the eastern part of an ocean basin when the easterly winds relax in the central part of the basin is discussed by Philander (1981) in a numerical model. These processes need to be studied in more detail especially in the eastern and central Pacific in order to determine what causes the low-frequency variation of SST. And we need to know whether the variations of SST in changing the surface saturation vapor pressure can independently cause the variations of moisture flux to the atmosphere.

In this paper we present the results of a study of the upper ocean heat budget using data from the Hawaii-to-Tahiti Shuttle Experiment. This study took place in the central Pacific Ocean (150–158°W) where 15 ship cruises were made, 14 of these between Hawaii (21°N) and Tahiti (17°S) from February 1979 to June 1980. The form of the heat budget is chosen in terms of the heat balance equation, vertically integrated from fixed deep isotherm depths to the sea surface so the contribution of the adiabatic motions to the heat budget is effectively filtered. As we shall see, the seasonal variation of the temperature averaged vertically in this manner closely corresponds to the seasonal variation of SST. The potentially important processes in this form of the heat budget are surface heat flux, heat storage rate, horizontal heat advection and vertical heat diffusion. The 16-month mean and seasonal variation of the surface heat flux were computed using empirical formulas and the standard meteorological data taken on board ship. The mean and seasonal variation of the heat storage rate were computed from the CTD data. Due to the noisiness of the horizontal heat advection estimates only values for the 16-month mean are statistically meaningful. No measurements of vertical diffusion were made.

The major results of this work are as follows. First, the surface heat flux plays a large role in determining the seasonal variation of SST. We conclude this because to a large extent the variations in heat storage rate are due to the surface heat flux (correlation coefficient of 0.70 between the two) and because the vertically averaged temperature (between fixed isotherms and the sea surface) is closely related to SST (i.e., the difference between the vertically averaged temperature and SST is small compared to the variation of SST). We do not see any correlation of the heat storage change with changes in horizontal advection. Second, there is no relation between isotherm depths in the upper part of the thermocline and SST. Therefore, at 150°W isentropic models of ocean circulation will not predict SST evolution during the FGGE shuttle period. Finally, the sea-surface temperature changes are not correlated (at zero phase) with latent heat flux from the ocean to the atmosphere; this implies there is no local feedback from the ocean to the atmosphere within the FGGE shuttle period.

In Section 2 the form of the upper ocean heat budget is derived and discussed. The data analysis is presented and discussed in Section 3. The surface heat flux results are presented in Section 4 while the heat storage rate and advection results are presented in Section 5. Finally, Section 6 covers the discussion and conclusions.

2. Upper-ocean heat budget

We wish to study the upper-ocean heat budget in such a way as to better understand the processes that affect the variation of SST. Near the ocean surface, the equations governing the conservation of heat and mass, respectively, are

$$\rho c\left(\frac{\partial T}{\partial t} + \mathbf{v}\cdot\nabla T + w\frac{\partial T}{\partial z}\right) = \frac{\partial q}{\partial z}, \tag{1a}$$

$$\nabla\cdot\mathbf{v} + \frac{\partial w}{\partial z} = 0, \tag{1b}$$

where T is temperature, $\mathbf{v}$ horizontal velocity, w vertical velocity, q vertical heat flux (sum of radiative and diffusive heat flux), ρc the specific heat capacity per unit volume, $\nabla \equiv (\partial/\partial x, \partial/\partial y)$ is the horizontal gradient, x, y and z are the eastward, northward and vertical coordinates respectively, and t is time. The horizontal diffusion of heat has been neglected.[2] By vertically integrating from the depth h of an isotherm to the sea surface the mass conservation equation becomes

$$w_{-h} + \mathbf{v}_{-h}\cdot\nabla h = \nabla\cdot h\mathbf{v}_a. \tag{2}$$

Here the subscript h indicates the velocities at depth h and $\mathbf{v}_a$ is the horizontal velocity averaged between depth h and the sea surface. The changes in mass due to precipitation and evaporation have been neglected. Using (1b) and (2) the heat conservation equation vertically integrated from depth h to the sea surface is

$$h\frac{\partial T_a}{\partial t} + h\mathbf{v}_a\cdot\nabla T_a + \nabla\cdot\left(\int_{-h}^{0}\hat{\mathbf{v}}\hat{T}dz\right) + (T_a - T_{-h}) \times\left(\frac{\partial h}{\partial t} + \mathbf{v}_{-h}\cdot\nabla h + w_{-h}\right) = Q - Q_{-h}, \tag{3}$$

where T_a is the temperature vertically averaged between depth h and the sea surface, $\hat{\mathbf{v}}$ is the deviation

[2] Recent estimates of horizontal eddy heat flux convergence show it to be as important as mean surface flux (Knox and Halpern, 1982, private communication), but we do not know how large the seasonal time-scale change is.

from the vertically averaged horizontal velocity ($\mathbf{v} = \mathbf{v}_a + \hat{\mathbf{v}}$), $\hat{T}$ is the deviation from the vertically averaged temperature ($T = T_a + \hat{T}$), Q the surface heat flux, and Q_{-h} the diffusive heat flux at depth h.

This form of the heat budget is used in order to filter out the effects of the vertical movements of the thermocline due to adiabatic motions of all frequencies (both high-frequency inertia–gravity waves and low-frequency planetary waves). In the shuttle data the thermocline typically moves up and down within a 25–75 m range. As an example, Fig. 1 shows the temperature profiles for each of the 15 cruises at 17°N, 158°W. At a constant temperature surface of depth h that is always within the main thermocline, less mixing is expected than in the surface mixed layer and therefore this surface is more nearly a material surface. Hence the term in (3) proportional to the entrainment rate ($\partial h/\partial t + \mathbf{v}_{-h} \cdot \nabla h + w_{-h}$) across the surface is minimized since the entrainment rate vanishes for a material surface. Within a degree or two of the equator, there is intense turbulence below the surface mixed layer due to the strong shear above the core of the equatorial undercurrent and vertical mixing, or entrainment, could still be important. On the other hand, the deeper the isotherm is the more the heat budget will reflect thermocline processes rather than upper-ocean processes. Therefore, the shallow isotherms which are always below the mixed layer are chosen.

Other researchers (e.g., Emery, 1976; Merle, 1980) have computed heat content to fixed depths. They have found that heat content to fixed depths is a useful way of measuring the redistribution of heat due to the vertical displacements of the main thermocline. We, however, wish to understand the processes that affect the low-frequency variation of SST. Fig. 2 shows that the temperature vertically averaged between the 24°C isotherm depth and the sea surface at 17°N, 158°W more closely corresponds to the SST variation than does the temperature vertically averaged between 100 m and the sea surface. Hence for purposes of understanding SST variation, studying the heat budget to isotherm depths is a better measure than the heat budget to fixed depths.

3. Data

The data used in this study were collected during the Hawaii-to-Tahiti Shuttle Experiment which took place from February 1979 to June 1980 in the central tropical Pacific Ocean. There were 15 cruises, 14 of which went between Hawaii and Tahiti. Each cruise (one way trip) took almost one month to complete. The R/V *Gyre* took the measurements on the first five cruises while the R/V *Wecoma* took the measurements on the last ten cruises. Fig. 3 shows the typical ship track between Hawaii and Tahiti, while Fig. 4 shows the noontime latitude of the ship as a function of time. For a more detailed description of the Shuttle Experiment, see Wyrtki *et al.* (1981).

Three separate data sets are used in this study: standard meteorological measurements, CTD data and profiling current meter data. First, the standard meteorological measurements (wind speed, air pressure, cloud amount, dry bulb temperature, wet bulb temperature and sea surface temperature) are used to compute the surface heat flux. These meteorological measurements were taken every six hours and while the ship was on station for a daily average of 5.3 observations, half of which were taken during daylight hours.

The net surface heat flux Q consists of the incoming shortwave solar radiation Q_S less the outgoing longwave radiation Q_B, latent heat flux Q_E and sensible heat flux Q_H:

$$Q = Q_S(1 - \alpha) - Q_B - Q_E - Q_H, \qquad (4)$$

where α is the surface albedo. Each component of the heat flux is estimated using a bulk formula. A detailed discussion of the formulas is presented in Stevenson (1982).

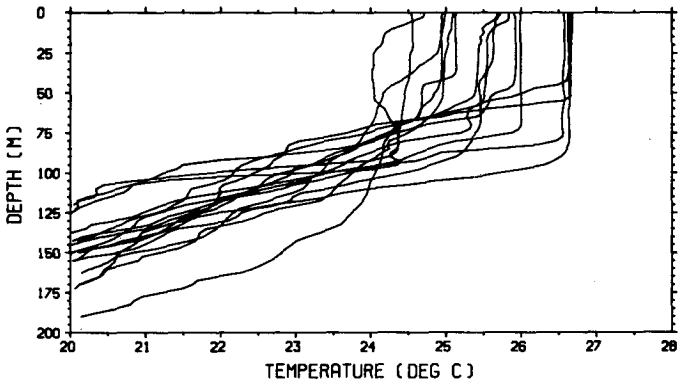

FIG. 1. Temperature profiles for each of the 15 cruises at 17°N, 158°W.

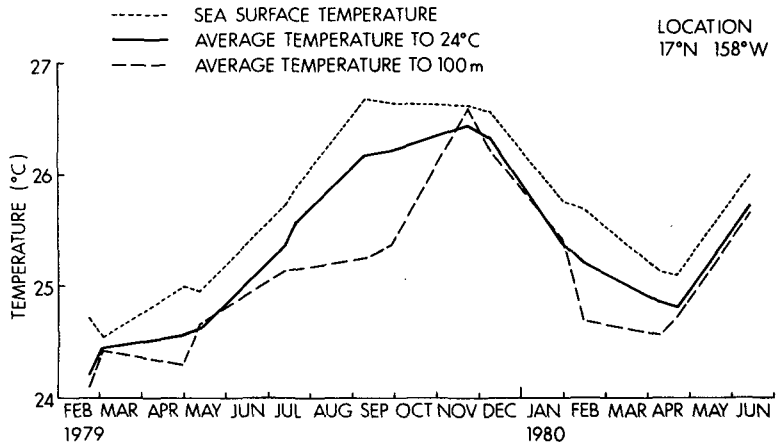

FIG. 2. Sea surface temperature, vertically averaged temperature to the 24°C isotherm depth, and vertically averaged temperature to the 100 m depth for each of the 15 cruises at 17°N, 158°W.

Here we present a brief summary of the formulas used. The shortwave solar radiation formula, which is an estimate of daily averaged radiation, is

$$Q_S = Q_{S_0}(1 - 0.62N_{\text{ave}} + 0.0019\alpha_s). \quad (5)$$

The clear-sky radiation Q_{S_0}, which is a function of latitude and time of year, is determined from a formula given by Seckel and Beaudry (1973). The term in parentheses is the cloud correction factor due to Reed (1977) where N_{ave} is the daytime-averaged cloud amount in tenths and α_s the noon altitude of the sun in degrees.

The formulas for longwave radiation, latent heat flux and sensible heat flux are all estimates of the instantaneous values of the fluxes as opposed to the daily estimate (5) of shortwave solar radiation. The formula for the longwave radiation, which is due to M.E. and T.G. Berliand (Budyko, 1974) is

$$Q_B = [\epsilon\sigma T_s^4(0.39 - 0.05e_{10}^{1/2}) + 4\epsilon\sigma T_s^3(T_s - T_{10})](1 - 0.7\text{N}), \quad (6)$$

where $\epsilon = 0.97$ is the emissivity of the sea surface, $\sigma = 5.673 \times 10^{-8}$ W m^{-2} K^{-4} is Stefan-Boltzmann's constant, e_{10} is the water vapor pressure (mb) at a height of 10 m, T_s the sea surface temperature (K), T_{10} the atmospheric temperature (K) at a height of 10 m, and N the fraction (tenths) of the sky that is covered by clouds. The factor $(1 - 0.7N)$ is the cloud correction factor suggested by Reed (1976) for the tropics.

The latent and sensible heat flux formulas are, respectively,

$$Q_E = \rho_a C_{E_{10}} L_E (q_s - q_{10}) U_{10}, \quad (7)$$

$$Q_H = \rho_a C_{P_a} \overline{w'T'} + 0.105\, Q_E, \quad (8a)$$

where

$$\overline{w'T'} = \begin{cases} 1.69 \times 10^{-3}\ ^\circ\text{C ms}^{-1} + 0.82 \times 10^{-3} U_{10}(T_s - T_{10}), & (T_s - T_{10}) < 0 \\ 2.24 \times 10^{-3}\ ^\circ\text{C ms}^{-1} + 1.12 \times 10^{-3} U_{10}(T_s - T_{10}), & (T_s - T_{10}) > 0, \end{cases} \quad (8b)$$

and ρ_a is the air density, $C_{E_{10}}$ the evaporation coefficient, L_E the latent heat of vaporization, q_s the specific humidity of saturated air at the sea surface temperature, q_{10} the specific humidity of the air at a height of 10 m, U_{10} the wind speed at a height of 10 m, C_{p_a} the heat capacity for dry air, and $\overline{w'T'}$ the vertical turbulent flux of temperature in the atmosphere. Eq. (8b) is suggested by Anderson and Smith (1981) where the first case is for a stable $(T_s - T_{10} < 0)$ atmosphere and the second for an unstable $(T_s - T_{10} > 0)$ atmosphere. As shown by Brook (1978) the term in (8a) proportional to the latent heat flux arises because the heat capacity for moist air depends on the specific humidity of the air.[3]

The bulk formulas (6), (7) and (8) are all applied at the standard height of 10 m above the sea surface. Since wind speed and wet and dry bulb temperatures were measured at different heights, the wind speed,

[3] While in press, Businger (1982) has pointed out that this is an erroneous correction, when total mass flux is considered. Therefore, our sensible plus latent flux estimates are about 10% too large. We thought it not worthwhile to change this computation.

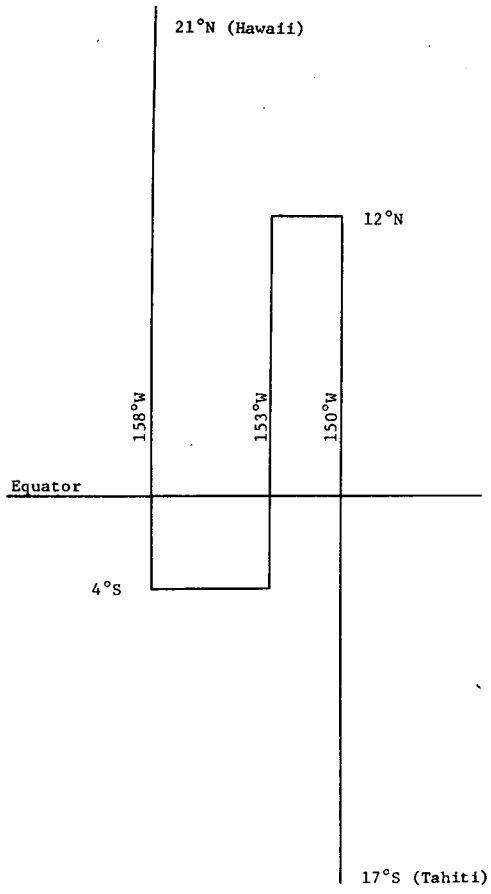

FIG. 3. Typical ship track between Hawaii and Tahiti.

humidity difference and air–sea temperature difference were all corrected to the 10 m height [see Stevenson (1982) for details]. These height corrections produced mostly less than 5% corrections in flux estimates. The neutral evaporation coefficient $C_{EN_{10}}$ [equal to 1.3×10^{-3} according to Friehe and Schmitt (1976) and Anderson and Smith (1981)] is increased on the average by 18% in correcting for stability to get the value of $C_{E_{10}}$ (Stevenson, 1982).

The heat flux estimates from individual ship observations have much high-frequency noise (typically 100 Wm^{-2}) as shown in Fig. 5. Therefore, a fair amount of averaging must be done to extract the seasonal signal. First, the longwave radiation, latent heat flux and sensible heat flux were daily averaged to be consistent with the daily averaged shortwave solar radiation. Second, the daily averages are averaged by cruise and latitude band. In other words, all the daily estimates within a given latitude range and cruise or pair of cruises are averaged together. There are eight latitude bands indicated on Fig. 4. Any daily value whose latitude at noon lies on a boundary between latitude bands is averaged with the values in the latitude band closer to the equator. In the northermost and southern two latitude bands all the daily values in pairs of cruises are averaged together, because of the small time differences between the cruises (cruises 1 and 2 through 13 and 14 and 15 by itself for the northernmost band, and 2 and 3 through 14 and 15 for the southern two bands). In all other latitude bands the daily values are averaged by single cruises. The result of the latitude-band averaging is eight time series of cruise means

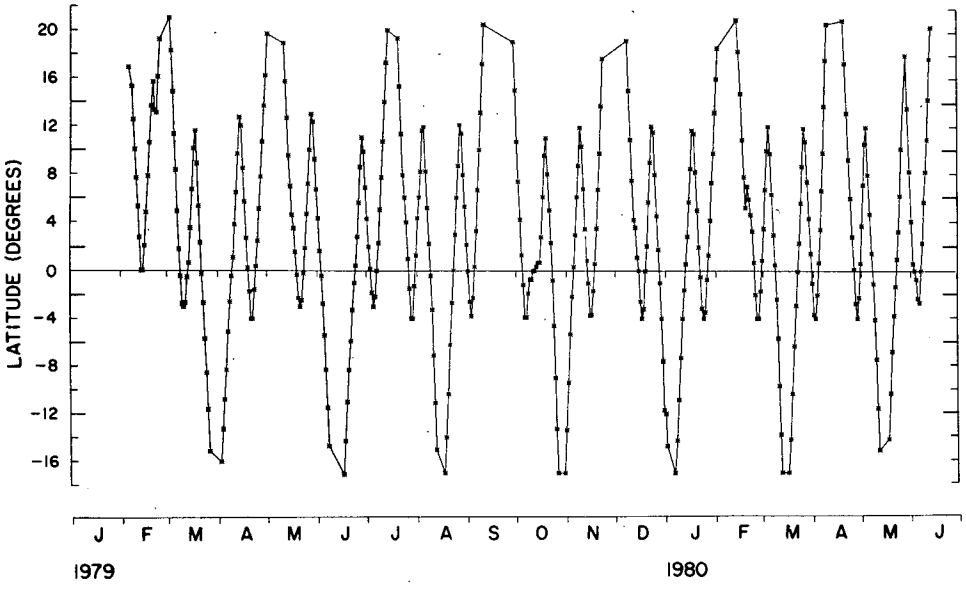

FIG. 4. Noontime latitude of the ship (indicated by asterisk) as a function of time. Heavy tick marks at 12°S, 6°S, 2°S, 2°N, 6°N, 10°N and 14°N indicate the latitude bands for averaging purposes.

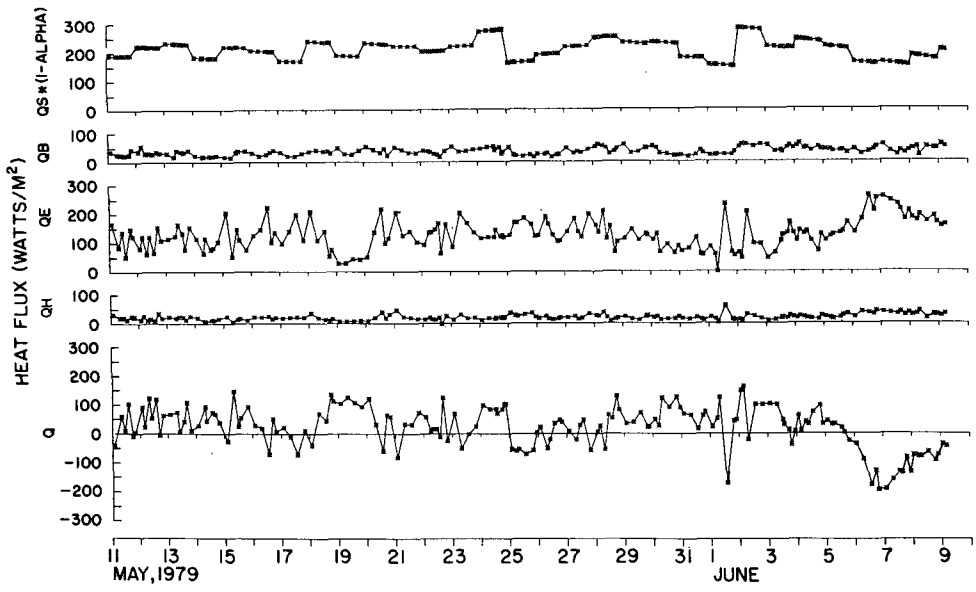

FIG. 5. Daily estimates of shortwave solar radiation and instantaneous estimates of longwave radiation, latent heat flux, sensible heat flux and net heat flux during cruise 4.

and variances, one for each latitude band. Finally each of these time series of means and variances is filtered using a ¼, ½, ¼ filter except the northernmost and southern two which are filtered using a ⅛, ¾, ⅛ filter. After all this averaging and smoothing we are left with the seasonal variation of the heat fluxes and the variance of the fluxes about the cruise means.

The second data set used in this study is the CTD data. The CTD profiles were taken to a depth of 1000 m at every degree of latitude and longitude along the ship track. The temperature profiles are used to compute rate of change in heat storage in the upper ocean. First the temperature is vertically averaged between the sea surface and an isotherm depth. The storage rate is then estimated by one of two methods. In the first method the storage rate is estimated at each location along the ship track by taking differences in vertically averaged temperature between consecutive cruises, dividing by the time interval between the occupations of the location, and multiplying by the average depth of the isotherm between the two occupations of the location. The storage rate estimates are averaged by cruise and latitute band and then filtered in time to isolate the seasonal variation as well as the variance about the cruise means in a manner identical to the treatment of the heat flux data. In the second method the vertically averaged temperatures, isotherm dpeths and times are first averaged by cruise and latitude band. Then the storage rate is estimated and filtered in time. The differences in heat storage rate estimates between these two methods are small.

The third data set is the PCM (profiling current meter) data taken by Firing *et al.* (1981). The current profiles were taken every degree along 158, 153 and 150°W between 10°N and 4°S and every half-degree between 3°N and 3°S. The current profiles along with the simultaneous temperature profiles taken by the same instrument are used to estimate horizontal heat advection. First the temperature and velocities are vertically averaged between the sea surface and the isotherm depth and the term $\int_{-h}^{0} \hat{v}\hat{T}dz$ is evaluated using the trapezoidal rule. Then the second term

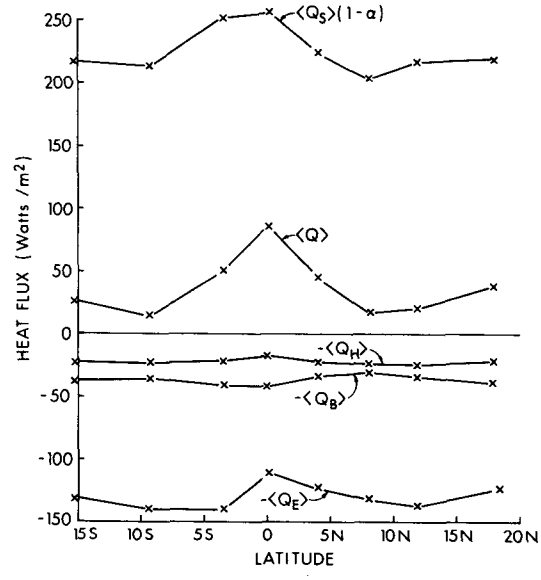

FIG. 6. Shortwave solar radiation, longwave radiation, latent heat flux, sensible heat flux and net heat flux averaged over all cruises. Angular brackets indicate 15-cruise means.

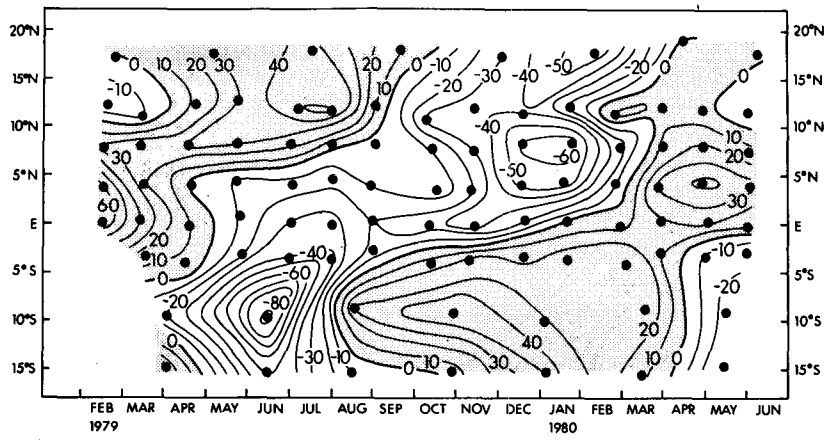

FIG. 7. Deviation Q' [W m^{-2}] of the net surface heat flux from the 15-cruise mean. Note primes indicate deviation from the mean and all of the latitude versus time plots have been averaged into the eight latitude bands and filtered in time.

(advection) and third term (divergence) of (3) are estimated for each cruise by taking the appropriate longitude and latitude differences. These terms are then averaged into the same latitude bands as the surface heat flux and storage terms. It is found that the data are too noisy to say anything about the seasonal variation of the horizontal heat advection. Hence only the mean of all 15 cruises as a function of latitude will be discussed.

4. Surface heat flux

The net surface heat flux with all its components averaged over all 15 cruises are shown in Fig. 6. There is a net positive heat flux into the ocean everywhere with a maximum of ~87 W m^{-2} at the equator. Climatological mean values of 40–50 W m^{-2} are reported by Weare *et al.* (1980) and Esbensen and Kushnir (1981). This maximum at the equator is due in part to greater incoming shortwave radiation which results from the clearer skies at the equator and in part to a minimum in latent heat flux at the equator. The latent heat flux minimum is due to both a lower mean wind speed and lower mean surface temperature at the equator.

The seasonal variation (with the 15-cruise mean removed) of the net surface heat flux is shown in Fig. 7, and the standard deviation about the cruise means is shown in Fig. 8. The heat flux varies from about 60 W m^{-2} to about −90 W m^{-2} with heating in the summer hemisphere and cooling in the winter hemisphere. This seasonal variation of the heat flux is mainly due to the seasonal variation of the shortwave solar radiation and the latent heat flux. The solar radiation variation (Fig. 9) tends to be more important to the north

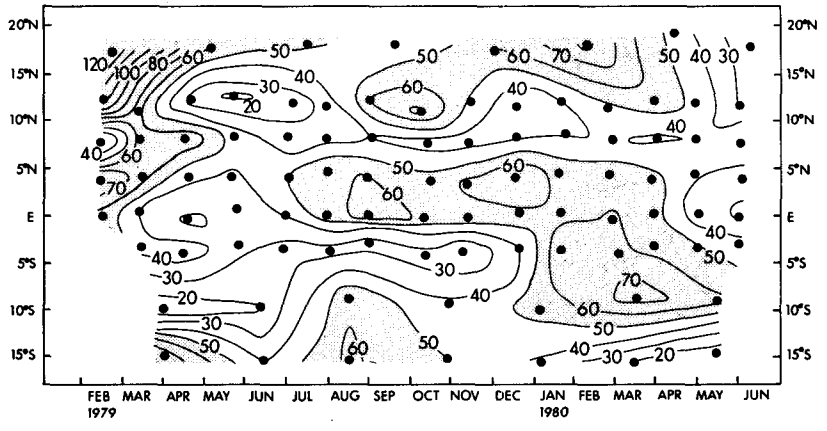

FIG. 8. Standard deviation (W m^{-2}) of the net surface heat flux.

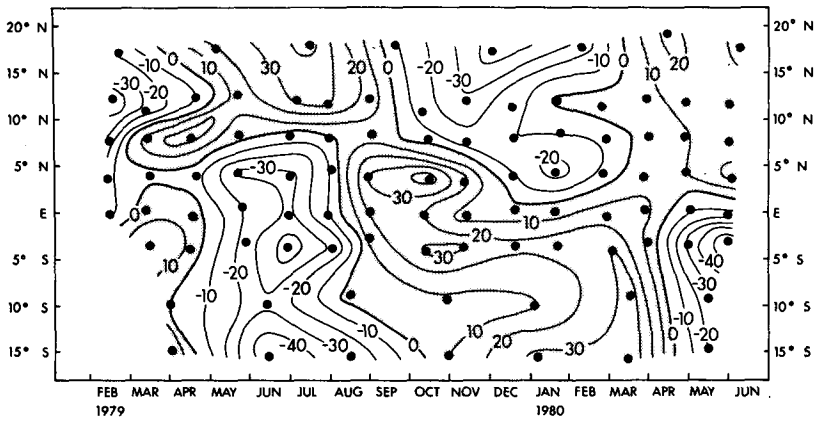

FIG. 9. Deviation $Q'_S(1 - \alpha)$ [W m^{-2}] of the shortwave solar radiation from the 15-cruise mean.

and south of the equator. The summertime heating and wintertime cooling around 15°N and the summertime heating between 5 and 15°S are mostly due to solar radiation. On the other hand, the latent heat flux variation (Fig. 10) tends to be more important closer to the equator. The heating at the equator in February 1979, the heating at 5°N in April and May 1980, the cooling between 5 and 10°N in December 1979 and January 1980, and the cooling at 10°S in June 1979 are primarily due to latent heat flux.

The seasonal variation of the shortwave solar radiation and the latent heat flux are due to several causes. Away from the equator the seasonal variation of the shortwave solar radiation (Fig. 9) is mainly due to the position of the sun (Fig. 11) while closer to the equator it is mainly due to the seasonal variation of cloudiness (Fig. 12). The seasonal variation of latent heat flux is caused by variation in wind speed and in humidity difference. Between 5 and 10°N in May and June 1979 and in December 1979 and January 1980 the respective minimum and maximum in latent heat flux (Fig. 10) are caused by variations in wind speed (Fig. 13). The maximum and minimum around 10°S in May and June 1979 and August and September 1979 respectively are also caused by variations in wind speed. On the other hand, between the equator and 5°N the seasonal variation of latent heat flux (minimum in February 1979, maximum in August, September and October 1979, and minimum in April and May 1980) is mainly due to the variation of humidity difference (Fig. 14). The seasonal variation of the humidity difference between the equator and 5°N is primarily due to the variation of the air specific humidity rather than the variation of the specific humidity of saturated air at the sea surface temperature. Off the equator, while the seasonal variation of both the air and the saturation humidity are as large as the seasonal variation of the air humidity at the equator, they are in phase and their difference is small. Apparently, off the equator the air is very nearly satu-

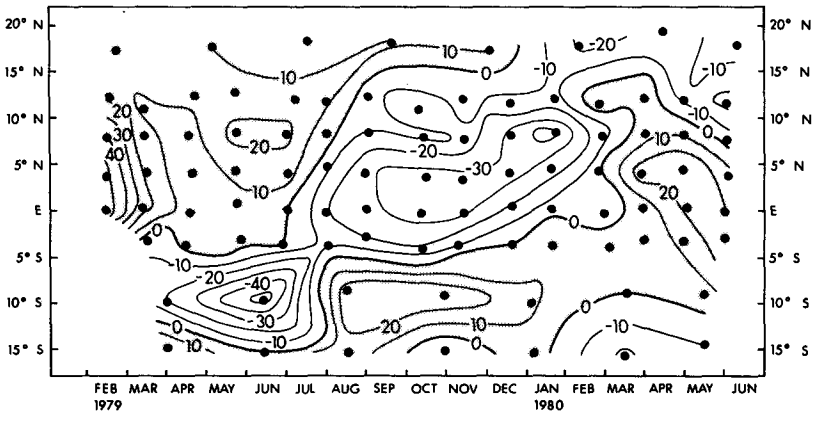

FIG. 10. Deviation Q'_E (W m^{-2}) of the latent heat flux from the 15-cruise mean.

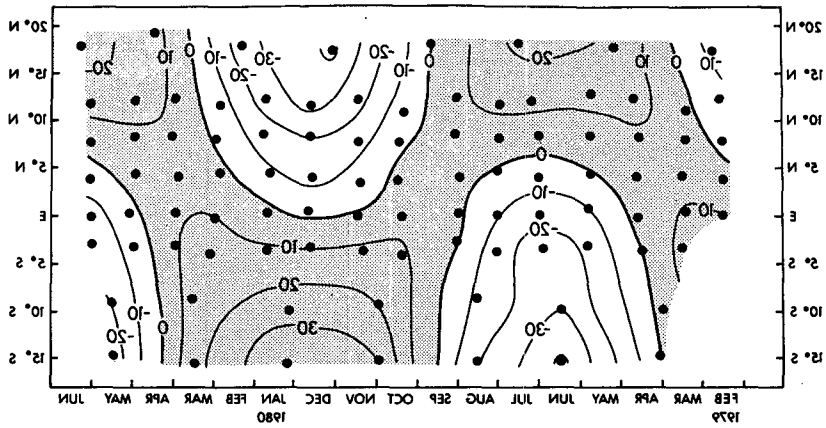

FIG. 11. Component $\langle f \rangle Q'_{S0}(1 - \alpha)$ [W m^{-2}] of the shortwave solar radiation due to the position of the sun where $f = 1 - 0.62\, N_{ave} + 0.0019\alpha_s$.

rated at air temperature. Hence during this experiment the ocean at the equator does not feed back locally to the atmosphere through a direct relationship between sea surface temperature and latent heat flux (also see Ramage and Hori, 1981).

5. Heat storage rate and advection

To what extent is the surface heat flux stored locally in the upper ocean hence affecting sea-surface temperature, and to what extent does horizontal heat advection affect the upper ocean heat balance? The 15-cruise means of surface heat flux Q, heat storage rate S, and horizontal heat advection A as a function of latitude are shown in Fig. 15. The horizontal heat advection A is the sum of the second and third terms of Eq. (3). The isotherms defining the lower boundaries of the upper-ocean region in which the heat storage and advection are estimated are 26.5°C between 6 and 2°S, 25.5°C between 2°S and 2°N, 26.0°C between 2 and 6°N, and 24.5°C between 6 and 10°N. The isotherms were chosen that were shallow but not ever within the surface mixed layer. A computation to the 24.0°C isotherm over the entire volume gave similar results. Table 1 shows the terms of the heat budget averaged from 6°S to 10°N and over all cruises. In addition to the heat storage, heat advection and surface heat flux we have made an estimate of the vertical diffusive heat flux Q_{-h} using the measured values of dissipation of turbulent kinetic energy obtained by Crawford and Osborn (1981) during January and February 1979. For details on how the diffusive heat flux is estimated see Niiler and Stevenson (1982). From Fig. 15 and Table 1 it is seen that the surface heat flux and horizontal heat advection are the largest components of the upper ocean heat budget when it is averaged over all 15 cruises. The storage rate tends to be less important. The diffusive heat flux estimate is quite uncertain since it was not

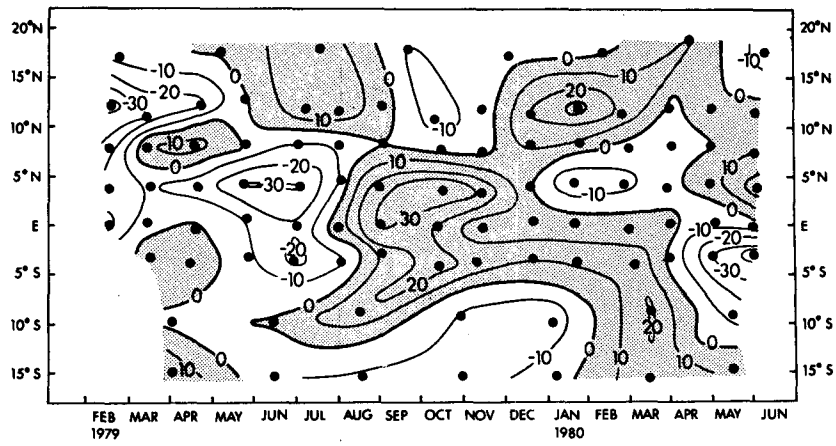

FIG. 12. Component $\langle Q_{S0} \rangle (1 - \alpha) f'$ [W m^{-2}] of the shortwave solar radiation due to the variation in cloudiness.

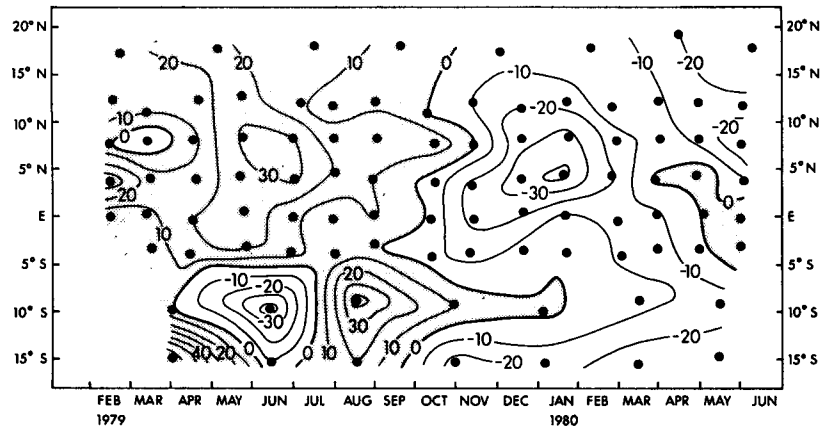

FIG. 13. Component $-\rho_a L_E \langle C_{E10} \rangle q_s - q_{10} \rangle U'_{10}$ [W m^{-2}] of the latent heat flux due to the variation in wind speed.

measured directly and was estimated from dissipation measurements made during only one cruise. The horizontal heat advection estimate is the most noisy computation, as shown by the standard deviation estimates on Fig. 15.

The seasonal variation of the heat storage rate computed by the second method is shown in Fig. 16. Computing the heat storage rate by the first method gives similar results. The isotherms defining the lower boundaries of the upper-ocean region in which the heat storage rate is estimated are shown in Table 2 for each latitude band. A computation of the heat storage rate using the 24.0°C surface as the lower boundary for the entire region produced similar results. Upon comparison with the surface heat flux (Fig. 7), it is seen that a good fraction of the surface heat flux on the seasonal time scale is stored locally in the upper ocean. The latitude–time correlation between the surface heat flux and heat storage rate is 0.70. The difference between the surface heat flux and the heat storage rate (shown in Fig. 17) must be due to horizontal heat advection, vertical heat diffusion, noise, or error. "Noise" is due to mesoscale fluctuations which we do not sample, while "error" is due largely to uncertainty of estimating the heat fluxes and the "errors" in estimating the currents with the shipborne profile method. The estimates of the horizontal heat advection are too noisy to say anything about its seasonal variation and the vertical heat diffusion was not measured. The standard deviations, or noise, of the surface heat flux (Fig. 8) and heat storage rate (Fig. 18) are certainly large enough to account for the difference. In particular, the difference is large in magnitude in March 1979 between 10 and 15°N, in January and February 1980 just north and south of the equator, and in April and May 1980 at and just south of the equator when the standard deviation of storage is large. We point out, how-

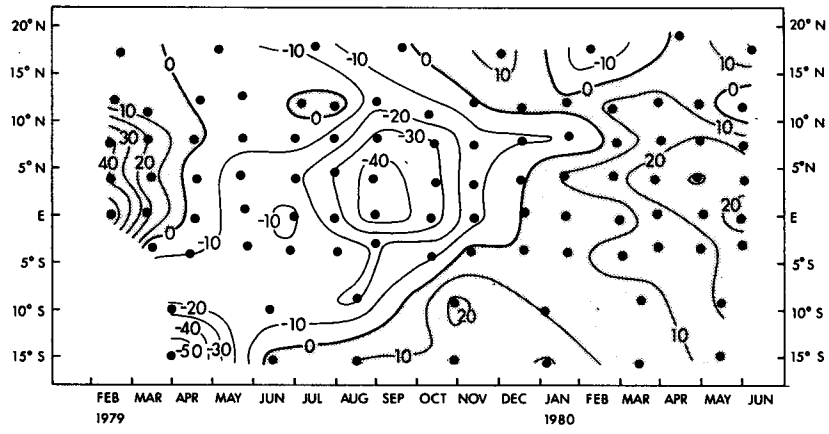

FIG. 14. Component $-\rho_a L_E \langle C_{E10} \rangle \langle U_{10} \rangle (q_s - q_{10})'$ [W m^{-2}] of the latent heat flux due to the variation of humidity difference.

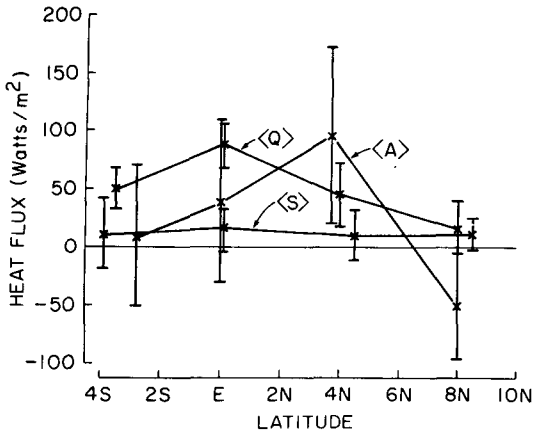

FIG. 15. Net surface heat flux $\langle Q \rangle$, horizontal heat advection $\langle A \rangle$ and local heat storage $\langle S \rangle$ averaged over all cruises. The error bars are the 95% confidence limits. The southernmost estimate of horizontal heat advection is the average of all the estimates between 4 and 2°S.

ever, that the 95% confidence limits for the cruise means of heat storage rate are as much as two times less than the standard deviations because 6–15 independent observations went into each cruise mean. On the other hand, the 95% confidence limits for the cruise means of surface heat flux are usually greater than the standard deviations because generally 2–6 independent observations (Fig. 4) went into each cruise mean.

The errors associated with the kind of bulk heat flux estimates we use are discussed by a number of investigators and range between 40–20 W m^{-2} (Bunker *et al.*, 1982). Whether these are random or bias errors is not presently known and cannot be ascertained from these data.

TABLE 1. Heat budget (W m^{-2}) averaged from 6°S to 10°N and over all cruises.

S	+	A	+	Q_h	=	Q
12(±10)		26(±32)		9–30		50(±12)

Note: Numbers within parentheses are 95% confidence limits.

6. Discussion and conclusions

Here we review our major findings. First, our most important conclusion is that in the central tropical Pacific Ocean at the time of the Hawaii-to-Tahiti Shuttle Experiment the surface heat flux plays a large role in the seasonal variation of the sea surface temperature. This is clearly seen in the comparison of Figs. 7 and 16. As shown in the previous section, much of the surface heat flux is stored locally in the upper ocean (0.70 correlation coefficient between surface heat flux and heat storage rate). Furthermore the seasonal variation of the temperature (Fig. 19) vertically averaged between the sea surface and the isotherms of Table 2 is quite similar (correlation coefficient of 0.97) but a little smaller than the seasonal variation of the SST. Therefore, most of the variability of SST can be modeled by simply storing the local heat flux into a variable mixed-layer depth.

Second, in our data we find no evidence for a correlation between shallow isotherm depths (Fig. 20) and cool SST as one would expect if a shallow thermocline made it easier for the turbulence to mix colder water to the surface. Furthermore, the difference between SST and the vertically averaged temperature is not smaller when the isotherms are shallower. Neither is there any correlation between surface heat flux minus heat storage rate and the depth of the main thermocline.

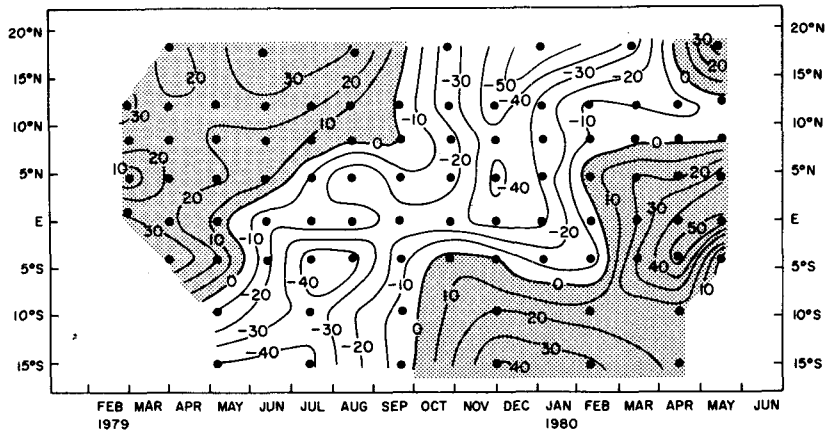

FIG. 16. Deviation S' (W m^{-2}) of the heat storage rate from the 15-cruise mean.

TABLE 2. Isotherm surface defining lower boundary for heat budget analysis.

Latitude	18°S, 12°S	12°S, 6°S	6°S, 2°S	2°S, 2°N	2°N, 6°N	6°N, 10°N	10°N, 14°N	14°N, 21°N
Isotherm	26.0°C	27.0°C	26.5°C	25.5°C	26.0°C	24.5°C	24.0°C	22.5°C

Third, computing vertically averaged temperatures (or heat content) to isotherm depths is more useful in understanding the variation of SST than computing vertically averaged temperatures to fixed depths. The vertically averaged temperature to 150 m shown in Fig. 21 is not correlated with the SST; however, it is well correlated (0.87) with the isotherm depths. Hence, heat content to fixed depths is useful for understanding how heat is moved around by vertical movements of the thermocline while heat content to isotherm depths is useful for understanding SST variation.

Fourth, at the time and location of this experiment there was no local feedback from the ocean to the atmosphere through a direct relationship between SST and latent heat flux. The seasonal variation of latent heat flux was primarily due to the seasonal variation of the wind speed and air humidity.

Fifth, the estimates of horizontal heat advection were too noisy to say anything about the effect of advection on the seasonal variation of SST. The mean of all 15 cruises indicates that horizontal heat advection is important on longer time scales and here water is cooled locally by it.

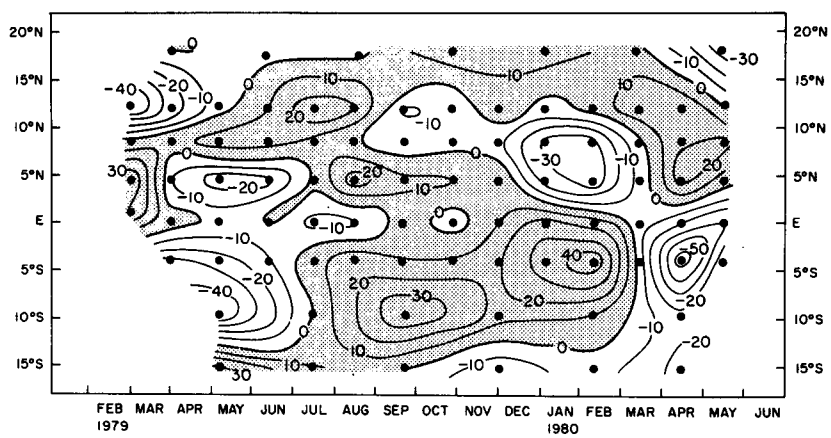

FIG. 17. Difference $Q' - S'$ (W m^{-2}) between the surface heat flux deviation and heat storage rate deviation from the 15-cruise mean.

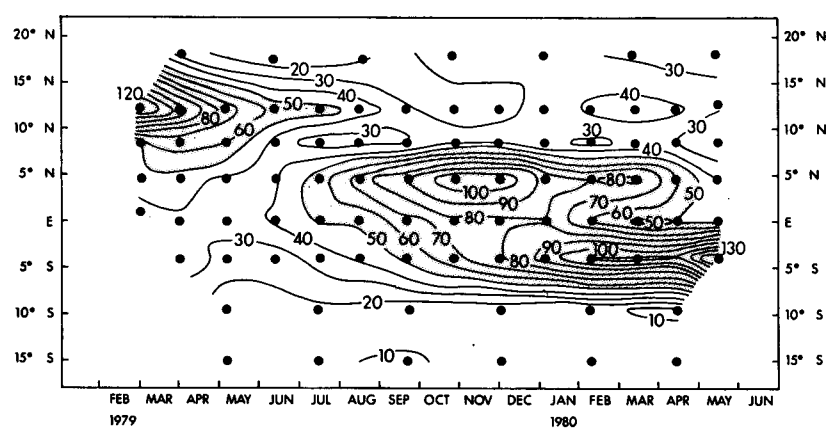

FIG. 18. Standard deviation (W m^{-2}) of the heat storage rate.

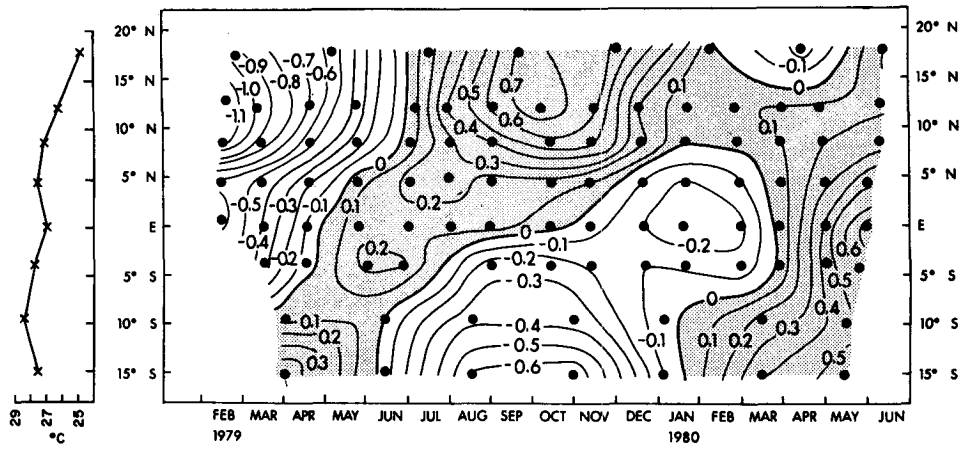

FIG. 19. Deviation T'_a (°C) of the vertically averaged temperature from the 15-cruise mean. On the left is the 15-cruise mean.

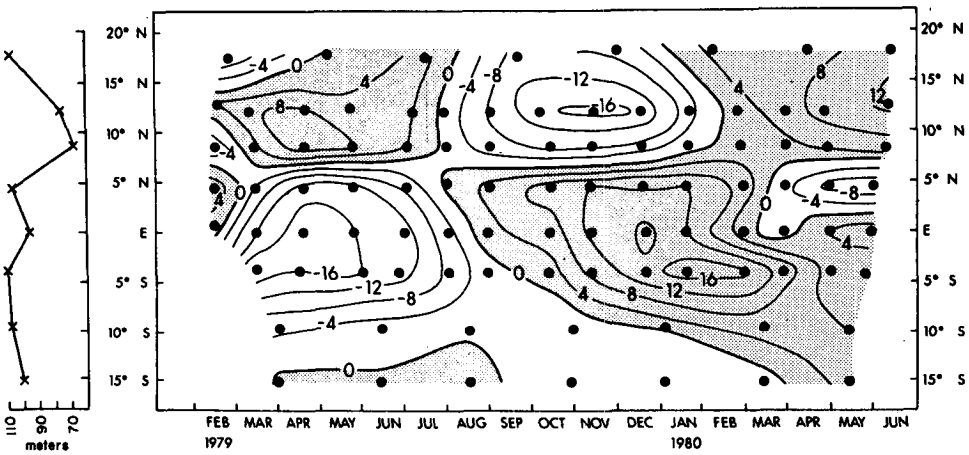

FIG. 20. Deviation h'(m) of the depth of the temperature surface from the 15-cruise mean. On the left is the 15-cruise mean.

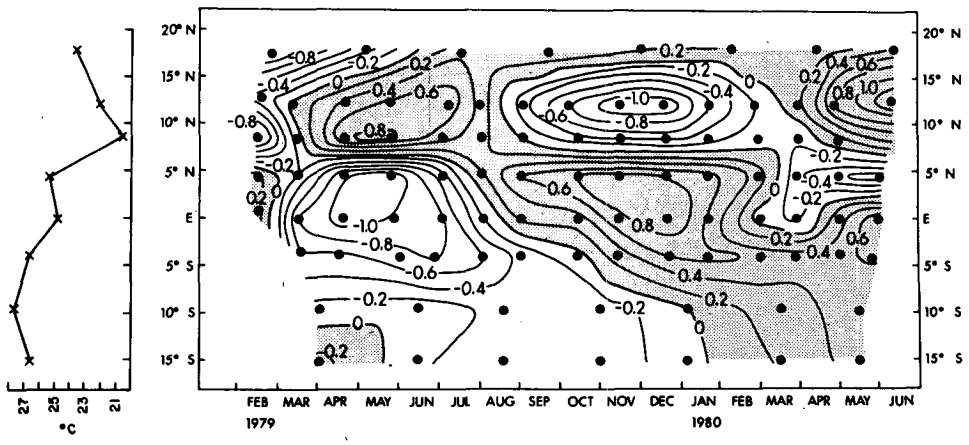

FIG. 21. Deviation T'_{150} (°C) of the vertically averaged temperature to 150 m from the 15-cruise mean. On the left is the 15-cruise mean.

Finally, it is important to study the upper ocean heat budget and turbulent mixing processes at other times (especially during warm anomalies or El Niños) and other regions such as the eastern tropical Pacific Ocean in order to better understand the processes that affect the low-frequency variation of SST. It is important to find out where, when and how SST feeds back to the atmosphere.

Acknowledgments. The valuable and able programming of Sharon Yokogawa is gratefully acknowledged. Klaus Wyrtki was very wise to have standard, high-quality meteorological data recorded on research vessels and we are grateful to Bernie Kilonsky for sharing the meteorological data logs and advice in interpreting these. Bruce Taft lent us the CTD data and Eric Firing provided his profiling current meter data and advice in its interpretation. Support of the Joint Institute for Marine and Atmospheric Research (JIMAR) through its Cooperative Agreement No. NA80RAH00002 between the University of Hawaii and the National Oceanic and Atmospheric Administration (Department of Commerce) is gratefully acknowledged.

REFERENCES

Anderson, R. J., and S. D. Smith, 1981: Evaporation coefficient for the sea surface from eddy flux measurements. *J. Geophys. Res.*, **86,** 449–456.

Barnett, T. P., 1981: Statistical prediction of North American air temperatures from Pacific predictors. *Mon. Wea. Rev.*, **109,** 1021–1041.

Brook, R. R., 1978: The influence of water vapor fluctuations on turbulent fluxes. *Bound.-Layer Meteor.*, **15,** 481–487.

Budyko, M. I., 1974: *Climate and Life.* Academic Press, 508 pp.

Bunker, A. F., H. Carnock and R. A. Goldsmith, 1982: A note on the heat balance of the Mediterranean and Red Seas. *J. Mar. Res.*, **40** (Suppl)., 73–83.

Busalacchi, A. J., and J. J. O'Brien, 1981: Interannual variability of the equatorial Pacific in the 1960's. *J. Geophys. Res.*, **86,** 10901–10907.

Businger, J. A., 1982: The fluxes of specific enthalpy, sensible heat and latent heat near the earth's surface. *J. Atmos. Sci.*, **39,** 1889–1892.

Crawford, W. R., and T. R. Osborn, 1981: Turbulence in the equatorial Pacific Ocean. PMSR81-1, Institute of Ocean Sciences, Sidney, B.C., Canada.

Davis, R. E., 1976: Predictability of sea surface temperature and sea level pressure anomalies over the North Pacific Ocean. *J. Phys. Oceanogr.*, **6,** 249–266.

——, 1978: Predictability of sea level pressure anomalies over the North Pacific Ocean. *J. Phys. Oceanogr.*, **8,** 233–246.

Emery, W., 1976: The role of vertical motion in the heat budget of the upper northeastern Pacific Ocean. *J. Phys. Oceanogr.*, **6,** 299–305.

Esbensen, S. K., and Y. Kushnir, 1981: The heat budget of the global ocean. Climate Research Institute., Rep. No. 29, Oregon State University, 305 pp.

Firing, E., C. Fenander and J. Miller, 1981: Profiling current meter measurements from the NORPAX Hawaii-to-Tahiti Shuttle Experiment. Hawaii Inst. Geophys. Rep. No. HIG-81-2, 146 pp.

Friehe, C. A., and K. F. Scmitt, 1976: Parameterization of air–sea interface fluxes of sensible heat and moisture by the bulk aerodynamic formulas. *J. Phys. Oceanogr.*, **6,** 801–809.

Horel, J. D., and J. M. Wallace, 1981: Planetary-scale atmospheric phenomena associated with the Southern Oscillation. *Mon. Wea. Rev.*, **109,** 813–829.

Hoskins, B. J., and D. J. Karoly, 1981: The steady linear response of a spherical atmosphere to thermal and orographic forcing. *J. Atmos. Sci.*, **38,** 1179–1196.

McPhaden, M. J., 1982: Variability in the central equatorial Indian Ocean, Part II: Oceanic heat and turbulent energy balances. *J. Mar. Res.*, **40,** 403–419.

Merle, J., 1980: Seasonal heat budget in the equatorial Atlantic Ocean. *J. Phys. Oceanogr.*, **10,** 464–469.

Newell, R. E., A. R. Navato and J. Hsiung, 1978: Long-term global sea surface temperature fluctuations and their possible influence on atmospheric CO_2 concentrations. *Pure Appl. Geophys.* **116,** 351–371.

Niiler, P. P., and J. W. Stevenson, 1982: The heat budget of tropical ocean warm water pools. *J. Mar. Res.*, **40** (Suppl.), 465–480.

Philander, S. G. H., 1981: The response of equatorial oceans to a relaxation of the trade winds. *J. Phys. Oceanogr.*, **11,** 176–189.

Ramage, C. S., and A. M. Hori, 1981: Meteorological aspects of El Niño. *Mon. Wea. Rev.*, **109,** 1827–1835.

Reed, R. K., 1976: On estimation of net long-wave radiation from the oceans. *J. Geophys. Res.*, **81,** 5793–5794.

——, 1977: On estimating insolation over the ocean. *J. Phys. Oceanogr.*, **7,** 482–485.

Seckel, G. R., and F. H. Beaudry, 1973: The radiation from sun and sky over the North Pacific Ocean (abstract). *Trans. Amer. Geophys. Union,* **54,** 1114.

Stevenson, J. W., 1982: Computation of heat and momentum fluxes at the sea surface during the Hawaii-to-Tahiti Shuttle Experiment. Hawaii Inst. Geophys. Rep. No. HIG-82-4, 42 pp.

Weare, B. C., P. T. Strub and M. D. Samuel, 1980: *Marine Climate Atlas of the Tropical Pacific Ocean. Contrib. Atmos. Sci.,* No. 20, University of California, Davis, 1–147.

Webster, P. J., 1981: Mechanisms determining the atmospheric response to sea surface temperature anomalies. *J. Atmos. Sci.*, **38,** 554–571.

Wyrtki, K., 1981: An estimate of equatorial upwelling in the Pacific. *J. Phys. Oceanogr.*, **11,** 1205–1214.

——, E. Firing, D. Halpern, R. Knox, G. J. McNally, W. C. Patzert, E. D. Stroup, B. A. Taft and R. Williams, 1981: The Hawaii-to-Tahiti Shuttle Experiment. *Science,* **211,** 22–28.